ELSEVIER

Journal of Crystal Growth 232 (2001) 273–284

JOURNAL OF CRYSTAL GROWTH

www.elsevier.com/locate/jcrysgro

Precision measurement of ternary diffusion coefficients and implications for protein crystal growth: lysozyme chloride in aqueous ammonium chloride at 25°C

Luigi Paduano[a,b], Onofrio Annunziata[a], Arne J. Pearlstein[c], Donald G. Miller[a,d], John G. Albright[a,*]

[a] *Department of Chemistry, Texas Christian University, Fort Worth, TX 76129, USA*

[b] *Dipartimento di Chimica, Università degli Studi di Napoli, Complesso Universitario Monte S. Angelo, Via Cinthia, 80126 Naples, Italy*

[c] *Department of Mechanical and Industrial Engineering, University of Illinois at Urbana-Champaign, 1206 West Green Street, Urbana, IL 61801, USA*

[d] *Geosciences and Environmental Technologies, Lawrence Livermore National Laboratory, P.O. Box 808, Livermore, CA 94551, USA*

Abstract

Isothermal ternary diffusion coefficients for the system lysozyme chloride (1) + NH_4Cl (2) + H_2O at 25°C and pH 4.5 have been measured interferometrically for five mean NH_4Cl concentrations, $C_2 = 0.25$, 0.5, 0.9, 1.2 and 1.5 M, with $C_1 = 0.6$ mM. The main-term diffusion coefficient $(D_{11})_v$ varies slowly with C_2. The main-term $(D_{22})_v$ increases with increasing NH_4Cl concentration, as does the binary D_v in aqueous NH_4Cl, but the $(D_{22})_v$ values are lower in the ternary system. The cross-term $(D_{21})_v$, which relates the coupled flow of NH_4Cl to the protein concentration gradient, increases sharply with increasing salt concentration, and is 19 times larger than $(D_{22})_v$ at the highest concentration. The values of $(D_{12})_v$ are smaller than the corresponding values previously obtained for the lysozyme chloride + NaCl + H_2O system over the whole range of salt concentration studied. Using equations based on the Onsager Reciprocal Relations, we have calculated the derivative of the chemical potential of lysozyme chloride with respect to the NH_4Cl concentration, and have estimated the protein cation charge. Integration with respect to the NH_4Cl concentration gives the dependence of the chemical potential of lysozyme chloride on NH_4Cl concentration, providing information about the driving force for nucleation and crystal growth of lysozyme chloride.

PACS: 36.20; 66.10; 81.10.Dn; 87.15.Da

Keywords: A1. Diffusion; A1. Mass transfer; A1. Multicomponent diffusion; A1. Supersaturated solutions; B1. Biological macro molecules; B1. Lysozyme; B1. Salts

1. Introduction

A large body of experimental and theoretical work has focused on the role of diffusion in protein crystal growth in multicomponent systems. These systems typically involve the desired protein, water, a salt precipitant, buffer, and sometimes a

*Corresponding author. Tel.: +1-817-257-6198; fax: +1-817-257-5851.

E-mail address: j.albright@tcu.edu (J.G. Albright).

0022-0248/01/$ - see front matter
PII: S0022-0248(01)01079-X

co-precipitant or impurities, including protein impurities. Diffusion is important in homogeneous and heterogeneous nucleation, as well as in crystal growth, where solution is typically depleted of protein in a boundary layer adjacent to the growing crystal [1–6]. In either case, a concentration gradient leads to diffusive transport, which under conditions of normal gravity can be accompanied by buoyancy-driven convection [5,6]. Under microgravity conditions, where convection is eliminated or at least suppressed, diffusion is the dominant transport mechanism [7], and should be faithfully modeled in order to predict the effects of growth conditions on crystal quality and growth rate.

To date, diffusive transport in protein crystal growth has been modeled using a simplified version of Fick's first law

$$\mathbf{J}_i = -D_i \nabla C_i, \tag{1}$$

which assumes that the flux of each solute is linearly proportional to the gradient of its own concentration. Here, $\mathbf{J}_i$ and D_i are the flux and pseudo-binary diffusion coefficient of the ith solute. In fact, it has been known since the 1950s that for many systems Eq. (1) is an inadequate description of the process, and must be replaced by

$$\mathbf{J}_i = -\sum_{j=1}^{n} D_{ij} \nabla C_j, \quad i = 1, \ldots, n. \tag{2}$$

Eq. (2) accounts for the fact that in an n-solute system, a gradient of one solute can lead to a flux of the other $n-1$ solutes [8]. The diagonal elements D_{ii} of the matrix of diffusion coefficients are called "main-term" diffusion coefficients, while the off-diagonal elements $D_{ij} (i \neq j)$ are referred to as "cross-term" coefficients. Eq. (2) is applicable in volume-fixed (subscript v), solvent-fixed (subscript 0), and other frames, with the understanding that the diffusion coefficients are not frame–invariant. The volume-fixed frame is usually a close approximation to the laboratory-fixed frame in which the diffusion coefficients are actually measured.

The thermodynamically more fundamental driving forces for diffusion are the chemical potential gradients, in terms of which Eq. (2) is equivalent to

$$(\mathbf{J}_i)_0 = -\sum_{j=1}^{n} (L_{ij})_0 \nabla \mu_j, \quad i = 1, \ldots, n, \tag{3}$$

where the $(L_{ij})_0$ are the so-called thermodynamic diffusion coefficients or "diffusion Onsager coefficients," and the chemical potential of the ith solute is μ_i. The subscript 0 refers to the solvent as well as the solvent-fixed reference frame, so that $(\mathbf{J}_0)_0 = 0$. The diffusion coefficients and thermodynamic diffusion coefficients in this frame are related through [9,10]

$$(D_{ij})_0 = \sum_{k=1}^{n} (L_{ik})_0 \frac{\partial \mu_k}{\partial C_j}, \quad i,j = 1, \ldots, n, \tag{4}$$

where the $(D_{ij})_0$ can be obtained from the measured volume-fixed $(D_{ij})_v$ using partial molar volumes [11]. In what follows, we denote the chemical potential derivatives by $\mu_{ij} = \partial \mu_i / \partial C_j$.

Experiment shows that the cross-term diffusion coefficients in an n-solute system can be positive or negative (e.g., [9,12,13]), and can have magnitudes comparable to or larger than the main-term coefficients [10,14]. Consequently, in the absence of information to the contrary, the full set of n^2 diffusion coefficients should be taken into account.

The full description (Eq. (2)) appears to be especially important for protein–salt–water systems. In two previous papers, for the lysozyme chloride (1) + NaCl (2) + H_2O system at pH 4.5 [14] and 6.0 [10], the cross-term diffusion coefficient $(D_{21})_v$ has been found to be much larger than both main-term diffusion coefficients $(D_{11})_v$ and $(D_{22})_v$, confirming the need to account for multicomponent effects when modeling transport during protein crystal growth.

Here we report precision diffusion coefficients for the ternary lysozyme chloride (1) + NH_4Cl (2) + H_2O system at 25°C and pH 4.5. This system is of considerable interest for two reasons. First, lysozyme is the prototypical globular protein used in crystal growth experiments in various aqueous electrolyte solutions. Its solubility, crystal growth, liquid–liquid phase transitions, and amorphous precipitation have been the subjects of several studies in aqueous NH_4Cl [15–17]. Second, given the complexity of protein crystal growth and the

considerable empiricism associated with the selection of favorable conditions for protein crystal growth, it is important to understand the variation of transport and thermodynamic effects for a series of salts with a common anion for growth of lysozyme.

We also use a new approach, first applied to lysozyme chloride (1) + NaCl (2) + H_2O systems at pH 4.5 and 6.0 [10], to calculate the derivative μ_{12} of the lysozyme chloride chemical potential with respect to NH_4Cl concentration, and then integrate to get the concentration dependence of the chemical potential of lysozyme chloride at 0.6 mM as a function of NH_4Cl concentration. Since the ternary diffusion measurements are possible well into the supersaturated region, the thermodynamic data are also available well beyond saturation. This allows the change of lysozyme chloride chemical potential to be determined well into the supersaturation region, and thus provides crucial information about the driving force for nucleation and crystal growth. The same μ_{ij} values allow us to estimate the charge on the protein [10].

2. Experimental procedure

The solution preparation procedures, apparatus, and density measurement procedures have been described earlier [14].

Six-times recrystallized hen egg-white lysozyme was purchased from Seikagaku America. Lot E96Y03 was used for all the experiments.

Molecular masses of water (M_0), lysozyme (M_1), and ammonium chloride (M_2) were taken to be 18.015, 14.307, and 53.496 g mol^{-1}, respectively. The ammonium chloride was Mallinckrodt AR grade, and was heated at 70°C for 7 h in a vaccum oven before use. Its crystal density was taken to be 1.527 g cm^{-3} for buoyancy corrections in weighing.

The diffusion coefficients were measured with the Gosting optical diffusiometer operating in its automated Rayleigh interferometry mode, using experimental procedures and data reduction techniques described earlier [14]. For each mean salt concentration, two diffusion experiments were performed for $\alpha_1 = 0$ and two for $\alpha_1 = 1$, where $\alpha_i \equiv R_i\Delta C_i/(R_1\Delta C_1 + R_2\Delta C_2)$ is the fraction of the refractive index difference between top and bottom solutions due to solute i, R_i is the refractive index increment of solute i (defined below), and ΔC_i is the concentration difference of solute i between the bottom and top solutions. The concentration differences were chosen to obtain $\sim$50 fringes in the Rayleigh fringe pattern.

3. Results

Ternary diffusion experiments were performed on the system lysozyme chloride + NH_4Cl + H_2O at mean NH_4Cl concentrations of 0.25, 0.5, 0.9, 1.2, and 1.5 M, with a single mean lysozyme chloride concentration of 0.6 mM. Data presented in Tables 1–5 include the mean concentrations $\bar{C}_i$

Table 1
Ternary experimental data at 25°C, [NH_4Cl] = 0.25 M

	H11	H12b	H13	H14
$\bar{C}_1$ (mM)	0.6000	0.6000	0.6000	0.6000
$\bar{C}_2$ (M)	0.2500	0.2500	0.2500	0.2500
ΔC_1 (mM)	0.4000	0.0000	0.4000	0.0000
ΔC_2 (M)	0.0000	0.1037	0.0000	0.1038
pH top	4.50	4.50	4.51	4.50
pH bottom	4.50	4.50	4.51	4.51
d (g cm^{-3}) top	1.002938	1.002902	1.002938	1.002887
d (g cm^{-3}) bottom	1.004592	1.004619	1.004597	1.004623
J (meas)	51.157	49.409	51.174	49.366
J (calc)	51.165	49.377	51.167	49.398
D_A (meas) (10^{-9} m^2 s^{-1})	0.1325	1.856	0.1328	1.851
D_A (calc) (10^{-9} m^2 s^{-1})	0.1326	1.865	0.1326	1.865

Table 2
Ternary experimental data at 25°C, [NH_4Cl] = 0.5 M

	H21b	H22	H23	H24
$\bar{C}_1$ (mM)	0.6000	0.6000	0.6000	0.6000
$\bar{C}_2$ (M)	0.5000	0.5000	0.5000	0.5000
ΔC_1 (mM)	0.4000	0.0000	0.4000	0.0000
ΔC_2 (M)	0.0000	0.1038	0.0000	0.1037
pH top	4.51	4.50	4.50	4.50
pH bottom	4.50	4.51	4.50	4.51
d ($g\,cm^{-3}$) top	1.007013	1.007001	1.007007	1.006993
d ($g\,cm^{-3}$) bottom	1.008649	1.008662	1.008646	1.008657
J (meas)	51.185	48.646	51.234	48.632
J (calc)	51.210	48.647	51.208	48.630
D_A (meas) ($10^{-9}\,m^2\,s^{-1}$)	0.1314	1.887	0.1311	1.887
D_A (calc) ($10^{-9}\,m^2\,s^{-1}$)	0.1313	1.901	0.1313	1.901

Table 3
Ternary experimental data at 25°C, [NH4Cl] = 0.9 M

	H31	H32	H33	H34
$\bar{C}_1$ (mM)	0.6000	0.6000	0.6000	0.6000
$\bar{C}_2$ (M)	0.9000	0.9000	0.9000	0.9000
ΔC_1 (mM)	0.3999	0.0000	0.3999	0.0000
ΔC_2 (M)	−0.0001	0.1083	0.0000	0.1083
pH top	4.50	4.50	4.50	4.50
pH bottom	4.50	4.50	4.50	4.50
d ($g\,cm^{-3}$) top	1.013312	1.013316	1.013312	1.013318
d ($g\,cm^{-3}$) bottom	1.014915	1.014971	1.014915	1.014967
J (meas)	51.254	49.835	51.199	49.831
J (calc)	51.217	49.830	51.227	49.836
D_A (meas) ($10^{-9}\,m^2\,s^{-1}$)	0.1318	1.936	0.1320	1.936
D_A (calc) ($10^{-9}\,m^2\,s^{-1}$)	0.1318	1.952	0.1319	1.952

Table 4
Ternary experimental data at 25°C, [NH_4Cl] = 1.2 M

	H41	H42	H43	H44
$\bar{C}_1$ (mM)	0.6000	0.6000	0.6000	0.6000
$\bar{C}_2$ (M)	1.2000	1.2000	1.1999	1.2000
ΔC_1 (mM)	0.4000	0.0000	0.3999	0.0000
ΔC_2 (M)	−0.0001	0.1084	0.0000	0.1084
pH top	4.51	4.51	4.51	4.50
pH bottom	4.50	4.50	4.50	4.50
d ($g\,cm^{-3}$) top	1.017914	1.017913	1.017896	1.017912
d ($g\,cm^{-3}$) bottom	1.019548	1.019546	1.019507	1.019576
J (meas)	51.171	49.268	51.141	49.281
J (calc)	51.155	49.283	51.157	49.266
D_A (meas) ($10^{-9}\,m^2\,s^{-1}$)	0.1333	1.978	0.1332	1.975
D_A (calc) ($10^{-9}\,m^2\,s^{-1}$)	0.1334	1.993	0.1334	1.993

Table 5
Ternary experimental data at 25°C, $[NH_4Cl] = 1.5\,M$

	H51c	H52b	H51b	H54
$\bar{C}_1$ (mM)	0.6000	0.6000	0.6000	0.6000
$\bar{C}_2$ (M)	1.4999	1.4999	1.4999	1.4999
ΔC_1 (mM)	0.4000	0.0000	0.3999	0.0000
ΔC_2 (M)	0.0000	0.1107	0.0000	0.1108
pH top	4.50	4.51	4.50	4.50
pH bottom	4.50	4.51	4.51	4.50
d ($g\,cm^{-3}$) top	1.022405	1.022411	1.022410	1.022426
d ($g\,cm^{-3}$) bottom	1.024026	1.024046	1.024031	1.024062
J (meas)	50.973	49.768	50.986	49.879
J (calc)	51.001	49.815	50.958	49.831
D_A (meas) ($10^{-9}\,m^2\,s^{-1}$)	0.1342	2.020	0.1341	2.018
D_A (calc) ($10^{-9}\,m^2\,s^{-1}$)	0.1342	2.034	0.1341	2.034

Table 6
Experimental diffusion coefficients and related data for the lysozyme chloride + NH_4Cl + water system at 25°C and pH 4.5

	H1	H2	H3	H4	H5
$\bar{\bar{C}}_1$ (mM)	0.6000	0.6000	0.6000	0.6000	0.6000
$\bar{\bar{C}}_2$ (M)	0.2500	0.5000	0.9000	1.2000	1.4999
$\bar{d}$ ($g\,cm^{-3}$)[a]	1.00376_3	1.00783_3	1.01412_8	1.01872_7	1.02322_7
H_1 ($g\,mol^{-1}$)	4141	4113	4012	4058	4058
H_2 ($g\,mol^{-1}$)	16.61	16.02	15.25	15.21	14.77
$\bar{V}_1$ ($cm^3\,mol^{-1}$)	10194	10221	10315	10269	10262
$\bar{V}_2$ ($cm^3\,mol^{-1}$)	36.986	37.569	38.317	38.355	38.773
$\bar{V}_0$ ($cm^3\,mol^{-1}$)	18.067	18.0628	18.051	18.050	18.040
R_1 ($10^2\,M^{-1}$)	1280	1280	1281	1280	1275
R_2 ($10^2\,M^{-1}$)	4.762	4.689	4.601	4.548	4.499
S_A/I_A	2.749	2.805	2.847	2.864	2.894
λ_1 ($10^{-9}\,m^2\,s^{-1}$)	0.1282	0.1244	0.1219	0.1208	0.1198
λ_2 ($10^{-9}\,m^2\,s^{-1}$)	1.826	1.844	1.891	1.930	1.969
$(D_{11})_v$ ($10^{-9}\,m^2\,s^{-1}$)	0.1283 ± 0.0001	0.1247 ± 0.0001	0.1224 ± 0.0001	0.1214 ± 0.0001	0.1206 ± 0.0001
$(D_{12})_v$ ($10^{-9}\,m^2\,s^{-1}$)	0.000025 ± 0.000001	0.000035 ± 0.000001	0.000036 ± 0.000001	0.000036 ± 0.000002	0.000037 ± 0.000001
$(D_{21})_v$ ($10^{-9}\,m^2\,s^{-1}$)	10.6 ± 0.1	16.9 ± 0.1	25.5 ± 0.2	33.0 ± 0.2	38.0 ± 0.2
$(D_{22})_v$ ($10^{-9}\,m^2\,s^{-1}$)	1.826 ± 0.001	1.844 ± 0.001	1.890 ± 0.001	1.930 ± 0.001	1.968 ± 0.001

[a] $\bar{d}$ refers to the values of $\bar{\bar{C}}_1$ and $\bar{\bar{C}}_2$ given in this table.

of both solutes; the concentration differences ΔC_i across the free-diffusion starting boundary at the starting time; the densities and pH values of top and bottom solutions; D_A, the reduced–height–area ratio [14]; the measured number of fringes J_{meas}; and J_{calc}. The values of J_{calc} were obtained from ΔC_i and refractive index increments with respect to J, $R_i = \partial J/\partial C_i$, which are proportional to the values of $R_i^* = \partial n/\partial C_i$, the increment with respect to the refractive index itself [10]. The values of J_{meas} and the corresponding ΔC_i were used to calculate the refractive index coefficients R_i [14].

Table 6 shows data derived from these five sets of experiments, including $\bar{C}_i$, the average of the mean concentrations, $\bar{C}_i$ of solute i in all solutions used in each series of four experiments at each mean composition; the partial molar volume $\bar{V}_i$ of the ith solute; the refractive index increments R_1 and R_2 of the solutes with respect to J; the diagnostic ratio S_A/I_A [14]; the eigenvalues λ_1 and

Table 7
Solvent-fixed Ternary Diffusion Coefficients for pH = 4.5

Series	H1	H2	H3	H4	H5
$\bar{C}_1$ (mM)	0.6000	0.6000	0.6000	0.6000	0.6000
$\bar{C}_2$ (M)	0.2500	0.5000	0.9000	1.2000	1.4999
$(D_{11})_0$ ($10^{-9}\,m^2\,s^{-1}$)	0.1293	0.1259	0.1238	0.1230	0.1223
$(D_{12})_0$ ($10^{-14}\,m^2\,s^{-1}$)	6.631	7.785	8.153	8.309	8.617
$(D_{21})_0$ ($10^{-9}\,m^2\,s^{-1}$)	11.0	17.9	27.6	36.2	42.3
$(D_{22})_0$ ($10^{-9}\,m^2\,s^{-1}$)	1.843	1.880	1.958	2.024	2.091

λ_2 ($\lambda_1 < \lambda_2$) of the matrix of diffusion coefficients; and the experimental diffusion coefficients $(D_{ij})_v$ relative to the volume-fixed frame of reference defined by

$$\sum_{i=0}^{n} (J_i)_v \bar{V}_i = 0, \tag{5}$$

where $(J_i)_v$ is the one-dimensional molar flux of the ith component in a volume-fixed frame. Finally, Table 6 shows, for each series of experiments, the parameters $\bar{d}$ and H_i obtained by least-squares fitting the equation

$$d = \bar{d} + H_1(C_1 - \bar{C}_1) + H_2(C_2 - \bar{C}_2) \tag{6}$$

to the densities of all solutions prepared for a series of experiments. (For some cases, identified by a literal suffix in Tables 1–5, densities of solutions prepared for unsuccessful diffusion experiments were included in the least-squares fits.) The H_i and $(D_{ij})_v$ were used to test for the static and dynamic stability of the diffusion boundary [18]. The boundaries were found to be stable in all cases. These values of H_1 and H_2 were also used to calculate the partial molar volumes $\bar{V}_i$ of the components, which were in turn used to convert volume fixed $(D_{ij})_v$ to the solvent-fixed values of $(D_{ij})_0$ shown in Table 7.

4. Discussion

For lysozyme chloride (1) + NH_4Cl (2) + H_2O at 25°C, pH 4.5, and 0.60 mM lysozyme chloride, Figs. 1(a–d) show the dependence (summarized numerically in Table 6) of the elements of the diffusion coefficient matrix on the NH_4Cl concentration. These are compared to corresponding values for the lysozyme chloride + NaCl + H_2O system at pH 4.5.

4.1. Examination of the D_{11} values

Fig. 1a shows that the lysozyme chloride main-term diffusion coefficient, $(D_{11})_v$, decreases much less rapidly with increasing NH_4Cl concentration than in the NaCl case. Fig. 1a suggests, as would be expected, that the limiting values of $(D_{11})_v$ coincide in the limit of vanishing salt concentration. We note that the values of $(D_{11})_v$ shown here are less than one-fifth of the corresponding binary lysozyme diffusion coefficients found without salt [10,14,19], and that considerably lower salt concentrations [19] are required to approach the binary value in these ternary systems.

4.2. Examination of the D_{12} values

Fig. 1(b) shows that the cross-term diffusion coefficient $(D_{12})_v$ (corresponding to the protein flux driven by a gradient of NH_4Cl concentration) is quite small. At low concentrations, it is nearly an order of magnitude smaller than in the NaCl ternary system. For $0.5\,M \leqslant C_2 \leqslant 1.5\,M$, $(D_{12})_v$ is essentially independent of NH_4Cl concentration, unlike the monotonically decreasing $(D_{12})_v$ for NaCl, and at each concentration is less than 50% of the NaCl value.

At low concentrations of either salt, a dominant factor is the long-range electrostatic interaction that enforces electroneutrality. As discussed in more detail in Section 4.6, this causes relatively immobile ions (e.g., lysozyme cation) to be pulled along by the electric field generated by the more

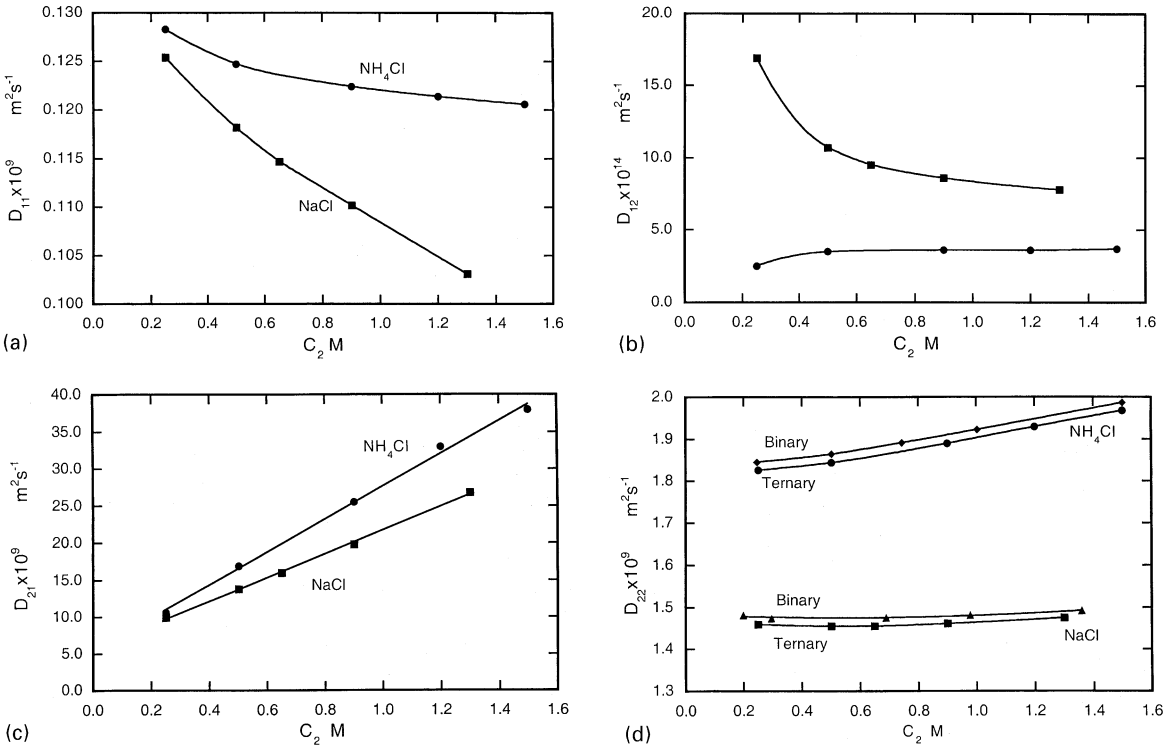

Fig. 1. Elements of the diffusion coefficient matrix for the ternary systems lysozyme chloride + NH_4Cl + water and lysozyme chloride + NaCl + water at pH 4.5 and 25°C: ● NH_4Cl, ■ NaCl. (a) D_{11}; (b) D_{12}; (c) D_{21}; (d) D_{22}: ◆ binary diffusion coefficient of NH_4Cl in water; ▲ binary diffusion coefficient of NaCl in water.

mobile ions (e.g., ammonium, sodium, and chloride).

For NH_4Cl concentrations in the range considered, the well-known Nernst–Hartley equations [8] predict a qualitatively *incorrect* dependence of $(D_{12})_v$ on NH_4Cl concentration, specifically that $(D_{12})_v$ decreases asymptotically to zero as C_2 increases at constant C_1. In fact, the measured values increase and plateau as C_2 increases. For NH_4Cl concentrations on the order of 0.1 M and higher, the calculated $(D_{12})_v$ are smaller than the experimental values. This is because short-range interactions become important at higher salt concentrations and keep the $(D_{12})_v$ values from approaching zero.

4.3. Examination of the D_{21} values

As can be seen from Table 6 and Fig. 1(c), the cross-term diffusion coefficient $(D_{21})_v$, which accounts for the flux of NH_4Cl due to a gradient of protein concentration, is very large and increases linearly with salt concentration. At the highest concentration considered ($C_2 = 1.5$ M), $(D_{21})_v$ is larger than both main-term diffusion coefficients, and more specifically, is about 19 times as large as $(D_{22})_v$. At 1.5 M NH_4Cl, the ratio $(D_{21})_v/(D_{11})_v$ is about 315. Consequently, the diffusion of each lysozyme cation is accompanied by a flux of 315 NH_4^+ and Cl^- ions, even when there is no overall NH_4Cl concentration gradient.

The aqueous ternary system studied here is composed of two electrolyte components with a common anion, Cl^-. The cation of one solute (lysozyme) is very large compared to that of the other. Thus, it is reasonable to expect the values of the diffusion coefficients to depend on (a) electrostatic interactions between the solutes, and (b) an "excluded volume effect" due to the reduction of volume available to the salt. As the NH_4Cl

concentration is increased, the excluded volume effect becomes the dominant influence on $(D_{21})_v$.

To better understand the excluded volume effect, consider a solution in which the salt concentration (in moles per unit volume of solution) is uniform but there is a gradient of lysozyme chloride. In the interstitial volume between lysozyme cations, the effective NH_4Cl concentration will exceed the nominal value, to an extent that will increase with increasing protein concentration. In this way, a gradient of lysozyme chloride will produce an "effective gradient" of NH_4Cl in the same direction. The resulting "effective" concentration gradient of NH_4Cl drives a flux of NH_4Cl, whose magnitude is related to the underlying protein concentration gradient by a constant of proportionality, $(D_{21})_v$.

4.4. Examination of the D_{22} values

Fig. 1(d) shows that the values of the main-term diffusion coefficient of NH_4Cl, $(D_{22})_v$, follow the same trend as the corresponding binary diffusion coefficients of NH_4Cl in H_2O [20], although the values are slightly lower. To a large extent, this result can be interpreted on the basis of obstruction of NH_4Cl diffusion by protein.

4.5. Examination of the determinant

Fig. 2 shows the NH_4Cl concentration dependence of the determinant $|\mathbf{D}|$ of the matrix of experimental diffusion coefficients. Theory shows [21–25] that at a spinodal point, this determinant must vanish. The determinant here is essentially constant, with a slight initial decrease with increasing NH_4Cl concentration being followed by an equally small increase at higher concentrations, unlike the determinant in the NaCl case, which decreases monotonically with salt concentration in the range considered [14]. If this behavior persists as the NH_4Cl concentration increases, one can conclude that a spinodal curve does not intersect the $C_1 = 0.6\,\mathrm{mM}$ line in the $C_1 - C_2$ plane.

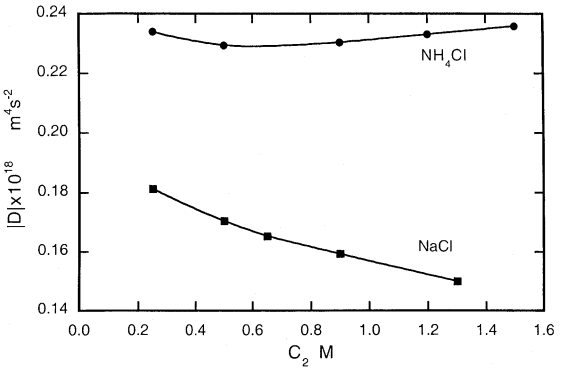

Fig. 2. Determinant of the diffusion coefficient matrix for the ternary system lysozyme chloride + NH_4Cl + water at pH 4.5 and 25°C: ● NH_4Cl, ■ NaCl.

4.6. Comparison with previous results for lysozyme chloride + NaCl + H_2O

Here, we compare the results of the present investigation to our earlier results for the lysozyme chloride + NaCl + H_2O system at pH 4.5 and 6.0 and the same lysozyme chloride concentration $C_1 = 0.6\,\mathrm{mM}$.

The main-term diffusion coefficient $(D_{11})_v$ decreases with salt concentration in the two ternary systems. However, its decrease is larger in aqueous NaCl ($\sim 17\%$) than in aqueous NH_4Cl ($\sim 5\%$). In general, since increasing the salt concentration reduces the electrostatic dragging effect of the chloride anion on the lysozyme cation, we expect a smooth decrease of the lysozyme chloride diffusion coefficient $(D_{11})_v$ for both systems.

We note that $(D_{11})_v$ in aqueous NH_4Cl is always larger than $(D_{11})_v$ in the NaCl system. This is probably due to the fact that the dynamic viscosity of binary $NH_4Cl + H_2O$ solutions initially decreases with increasing NH_4Cl concentration (up to 2.0 M at 25°C), and does not greatly increase at higher concentrations [26]. On the other hand, the dynamic viscosity of aqueous NaCl solutions increases monotonically with NaCl concentration. The result is that the slowing effect of viscosity on lysozyme chloride diffusion is more pronounced in aqueous NaCl than in NH_4Cl.

Direct comparison of the main-term diffusion coefficients $(D_{22})_v$ for the two systems is

complicated by the fact that the two salts are characterized by different physicochemical properties (e.g., transference numbers, activity coefficients, conductivities). For both cases, however, the values of $(D_{22})_v$ lie no more than 1–2% below the corresponding binary diffusion coefficients over the entire range of composition. The slightly lower values of the ternary $(D_{22})_v$ are accounted for in part by protein obstruction, which is expected to have effects of nearly identical magnitude for the two salts.

The cross-term diffusion coefficients $(D_{21})_v$ increase rapidly with salt concentration for both systems. For an NH_4Cl concentration of 1.2 M, $(D_{21})_v$ reaches a value about 20% higher than the corresponding cross-term for the NaCl system. This is reasonable because, although $(D_{21})_v$ is dominated by the excluded volume effect due to lysozyme chloride (solute 1), which is common to both systems, its magnitude also depends on diffusion of salt (solute 2) in the interstitial solution. Thus, we expect that the solute with the higher diffusion coefficient, NH_4Cl, will give rise to a larger $(D_{21})_v$ value than the more slowly diffusing NaCl.

Comparison of the diffusion coefficients is perhaps most interesting for $(D_{12})_v$. At low salt concentrations, the difference between the mobilities of the salt's cation and anion becomes critical to interpretation of the data. At low salt concentrations, the electric field associated with the difference in mobilities of the salt cations and anions pulls the lysozyme cations. However, the ionic mobility of NH_4^+ is nearly equal to that of Cl^-, so that only a weak field is generated by diffusion of NH_4Cl, and there is little "pull" on the lysozyme cations. Thus, at low salt concentrations, $(D_{12})_v$ in NH_4Cl solution is much smaller than in aqueous NaCl, for which the difference between cation and anion mobilities is much larger.

The fact that the determinant $|\mathbf{D}|$ for the lysozyme chloride + NH_4Cl + H_2O system is 13–25% larger than that for the corresponding NaCl system is largely accounted for by the larger $(D_{22})_v$ value for NH_4Cl.

5. Use of irreversible thermodynamics and diffusion data to obtain chemical potential derivatives

Evaluation of the chemical potential derivative of each solute with respect to the other has been described earlier [10]. The approach, which in the ternary case is limited to systems in which the molar concentration of one solute is very small compared to that of the other, is based on a) equality of the cross-derivatives of the chemical potential with respect to *molality* according to

$$\frac{\partial \mu_1}{\partial m_2} = \frac{\partial \mu_2}{\partial m_1}, \tag{7}$$

which becomes

$$\begin{aligned}\frac{1}{C_0 M_0}\frac{\partial \mu_1}{\partial m_2} &= \mu_{12}(1 - C_2\bar{V}_2) - \mu_{11}C_1\bar{V}_2 \\ &= \mu_{21}(1 - C_1\bar{V}_1) - \mu_{22}C_2\bar{V}_1 \\ &= \frac{1}{C_0 M_0}\frac{\partial \mu_2}{\partial m_1}\end{aligned} \tag{8}$$

in terms of derivatives with respect to *molarity*, and (b) the Onsager Reciprocal Relations, which correspond to equality of the cross-thermodynamic transport coefficients in the solvent-fixed reference frame

$$\begin{aligned}(L_{12})_0 &= \mu_{11}(D_{12})_0 - \mu_{12}(D_{11})_0 \\ &= \mu_{22}(D_{21})_0 - \mu_{21}(D_{22})_0 = (L_{21})_0.\end{aligned} \tag{9}$$

Using Eqs. (3) and (9), we obtain the following expressions for the molarity cross-derivatives

$$\mu_{12} = \frac{\mu_{11}[C_1\bar{V}_2(D_{22})_0 - (1 - C_1\bar{V}_1)(D_{12})_0] - \mu_{22}[C_2\bar{V}_1(D_{22})_0 - (1 - C_1\bar{V}_1)(D_{21})_0]}{(1 - C_2\bar{V}_2)(D_{22})_0 - (1 - C_1\bar{V}_1)(D_{11})_0}, \tag{10a}$$

$$\mu_{21} = \frac{\mu_{11}[C_1\bar{V}_2(D_{11})_0 - (1 - C_2\bar{V}_2)(D_{12})_0] - \mu_{22}[C_2\bar{V}_1(D_{11})_0 - (1 - C_2\bar{V}_2)(D_{21})_0]}{(1 - C_2\bar{V}_2)(D_{22})_0 - (1 - C_1\bar{V}_1)(D_{11})_0}. \tag{10b}$$

Hence, μ_{12} and μ_{21} are simply related to the self-derivatives μ_{11} and μ_{22} and the four measured elements of the diffusion coefficient matrix.

Using the general thermodynamic expression for the chemical potential of each solute in terms of molarity and mean ionic activity coefficients y_i, and taking the stoichiometric coefficients for the cations to be unity, we find the following relationships, written in matrix form:

$$\begin{bmatrix} \mu_{11} & \mu_{12} \\ \mu_{21} & \mu_{22} \end{bmatrix} = RT \begin{bmatrix} \dfrac{1}{C_1} + \dfrac{z_P^2}{N} + (z_P+1)\dfrac{\partial \ln y_1}{\partial C_1} & \dfrac{z_P}{N} + (z_P+1)\dfrac{\partial \ln y_1}{\partial C_2} \\ \dfrac{z_P}{N} + 2\dfrac{\partial \ln y_2}{\partial C_1} & \dfrac{1}{C_2} + \dfrac{1}{N} + 2\dfrac{\partial \ln y_2}{\partial C_2} \end{bmatrix}. \tag{11}$$

Here, z_P is the absolute charge on the protein cation, and we have used $z_{Cl} = 1$ and $z_{NH_4} = 1$ for the absolute values of the charges of the chloride anions common to the two solutes and the ammonium cation, respectively. Note that $N = z_P C_1 + C_2$ is equivalent to the total normality of the ternary solution.

Eqs. (10a) and (10b) require values of μ_{11} and μ_{22}. From Eq. (11), we obtain

$$\mu_{11} = \frac{RT}{C_1}\left[1 + \frac{z_P^2 C_1}{z_P C_1 + C_2} + (z_P+1)C_1\frac{\partial \ln y_1}{\partial C_1}\right]. \tag{12}$$

For very low values of C_1, the bracketed factor on the right-hand side of Eq. (12) is dominated by the first two terms, and for 0.6 mM lysozyme chloride in NaCl, the error associated with dropping the third term does not exceed 10% [10].

A good value of μ_{22} can be obtained from binary activity data for aqueous NH_4Cl. It is seen that the concentration dependence of $(D_{22})_v$ closely follows that of the corresponding binary diffusion coefficient over the entire range of NH_4Cl concentration. Since diffusion coefficients depend on the thermodynamic driving force, the close similarity in the concentration dependence of the diffusion coefficients suggests that it is reasonable to approximate $\partial \ln y_2/\partial C_2$ in the ternary system by its binary value. The binary salt concentration used for this calculation should be the same as the interstitial $NH_4^+ + Cl^-$ ionic strength in the ternary system. Taking advantage of the fact that $z_{NH_4} = z_{Cl} = 1$, μ_{22} can be rewritten as

$$\mu_{22} = \frac{RT}{C_2}\left[1 + \frac{C_2}{z_P C_1 + C_2} + 2C_2\left(\frac{\partial \ln y_2}{\partial C_2}\right)_{\text{binary}}\right]. \tag{13}$$

Eqs. (10a) and (10b) can now be used to obtain μ_{12} and μ_{21}, whose values are reported in Table 8.

It is important to note that the contributions of the μ_{11} to Eqs. (10a) and (10b) are relatively small, so that even a 10–20% error in μ_{11} will contribute negligibly to error in the calculated μ_{12} and μ_{21}. The dominant terms in Eqs. (10a) and (10b) are μ_{22} and D_{21}. The overall error in the calculated μ_{12} and μ_{21} is estimated to be less than 5%.

The values of μ_{12} and μ_{21}, as mentioned above, can be used to calculate the protein charge and the change of the lysozyme chloride chemical potential with NH_4Cl concentration. If the saturation concentration is taken as the reference state, the chemical potential change from this reference

Table 8
Chemical Potentials and Derivatives for pH = 4.5

C_2 (M)	μ_{11}/RT (M^{-1})	μ_{22}/RT (M^{-1})	μ_{12}/RT (M^{-1})	μ_{21}/RT (M^{-1})	$(\mu_1 - \mu_1^*)/RT$
0.2500	1743	7.163	26.4	44.6	−10.45
0.5000	1705	3.615	17.1	35.4	−5.14
0.9000	1682	1.587	10.8	29.7	0
1.2000	1679	1.305	9.6	28.9	2.86
1.4999	1688	2.064	7.0	26.8	5.30

value will give the driving force for protein nucleation and crystal growth.

6. Use of μ_{12} and μ_{21} to calculate the relative chemical potential of lysozyme chloride

We must first estimate the charge on the lysozyme cation. The expressions given in Eq. (11) for the cross-derivatives indicate how μ_{12} and μ_{21} can be used to calculate it. If we multiply μ_{12} and μ_{21} by the normality $N = z_P C_1 + C_2$, assume that the activity coefficient derivatives are constant, e.g., $\partial \ln y_i/\partial C_j = a_{ij}$, we can then rewrite the expressions for μ_{12} and μ_{21} as

$$Y_{12} = (z_P C_1 + C_2)\frac{\mu_{12}}{RT} = z_P + a_{12}(z_P + 1)(z_P C_1 + C_2), \quad (14a)$$

$$Y_{21} = (z_P C_1 + C_2)\frac{\mu_{21}}{RT} = z_P + 2a_{21}(z_P C_1 + C_2). \quad (14b)$$

Nonlinear least-squares fits of Eqs. (14a) and (14b) to the previously calculated $\mu_{ij}\,(i \neq j)$ allow the parameters a_{12} and a_{21} and the protein charge z_P to be determined. The fitted z_P values obtained are 6.55 and 5.78, corresponding to $a_{12} = 0.434\,M^{-1}$ and $a_{21} = 11.68\,M^{-1}$, respectively. The values of μ_{12} and μ_{21} depend on μ_{11}, and hence on the assumed charge. An iteration shows that this effect is small and can be ignored. Note that nonlinear least-squares calculations of a_{12}, a_{21}, and z_P performed for different arrangements of Eqs. (14a) and (14b) correspond to different weightings of the sum of the squared errors, and can give somewhat different results.

These fitted z_P values can be compared to $z_P \approx 12$ [27], obtained from pH titration measurements. The titration measurements give no indication of chloride anion association with the lysozyme cation. Such association will have the effect of reducing the protein charge.

Integrating Eq. (14a) permits calculation of the chemical potential of lysozyme chloride as a function of NH_4Cl concentration at fixed lysozyme chloride concentration. The integral can be written as

$$\mu_1 - \mu_1^* = \int \mu_{12} dC_2 = RT\left\{ z_P \ln\frac{z_P C_1 + C_2}{z_P C_1 + C_{2,s}} + a_{12}(z_P + 1)(C_2 - C_{2,s})\right\}, \quad (15)$$

where we have used $z_P = 6.55$ and $a_{12} = 0.434\,M^{-1}$. Here, $C_{2,s}$ corresponds to the NH_4Cl concentration at which lysozyme chloride in solution is in equilibrium with crystalline tetragonal lysozyme. Besides a single measurement for 0.3 M NH_4Cl in a two-buffer system, the only solubility data known to us for lysozyme chloride in aqueous NH_4Cl is in acetate-buffered solution at 18°C [15]. Thus, we have arbitrarily chosen 0.9 M as the reference state in order to directly compare changes of the lysozyme chloride chemical potential to those previously reported for NaCl.

The derivative of the chemical potential of the lysozyme chloride is about 20% less than in the NaCl case. We note that these results depend on the model chosen (Eqs. 14a and 14b). If, for example, binding of ammonium cations to the protein were important at higher NH_4Cl concentrations, the model would require modification.

Values of the chemical potential of lysozyme chloride, relative to the $C_2 = 0.9$ M reference state, are shown in Table 8. This dependence of the chemical potential (referred to the same reference state) on NH_4Cl concentration is shown in Fig. 3.

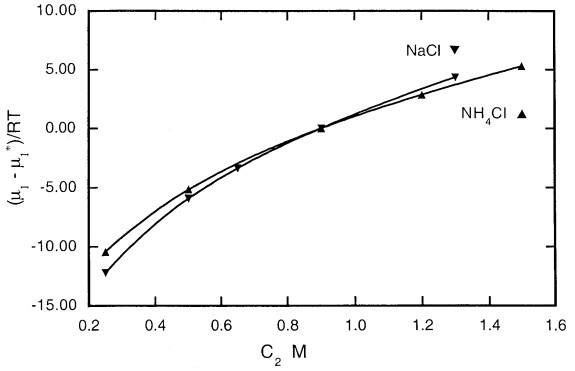

Fig. 3. Integrated values of chemical potential derivatives $(\mu_1 - \mu_1^*)/RT$ versus C_2 at pH 4.5 and 25°C: ▲ NH_4Cl, ▼ NaCl.

We are aware of only one previous set of measurements of the derivative of the chemical potential of lysozyme prior to our recent work [10]. Arakawa and Timasheff [28] derived values of the molal derivative ($\partial\mu_1/\partial m_2$ in our notation) from density measurements, and reported $\partial\mu_1/\partial m_2$ for lysozyme in 1.0 M solutions of sodium chloride, magnesium chloride, magnesium acetate, and magnesium sulfate. Each solution was buffered, and the pH was 4.5 in all but the magnesium acetate case, for which it was 5.6. Using Eq. (8) and our tabulated values of μ_{11} and μ_{12}, linearly interpolated to 1.0 M NH_4Cl, we find $\partial\mu_1/\partial m_2 = 5.63\,\mathrm{kcal\,mol^{-1}(mol\,kg^{-1})}$ for the derivative of the lysozyme chloride chemical potential with respect to NH_4Cl molality. The range 4.0–6.8 $\mathrm{kcal\,mol^{-1}/(mol\,kg^{-1})}$ obtained by Arakawa and Timasheff with different electrolytes [28] is in good qualitative agreement with our value. (The derivative with respect to NaCl molality obtained by Arakawa and Timasheff [28] is $6.8 \pm 1.7\,\mathrm{kcal\,mol^{-1}/(mol\,kg^{-1})}$, which compares well to our value of $6.37\,\mathrm{kcal\,mol^{-1}/(mol\,kg^{-1})}$.)

7. Conclusions

We have now reported precision measurements of ternary diffusion coefficients in a second aqueous lysozyme chloride system. The present results clearly demonstrate the capability to obtain high-precision ternary diffusion coefficients in aqueous protein solutions. The magnitude of the cross-term diffusion coefficient $(D_{21})_v$, which is about 19 times the magnitude of the diagonal term $(D_{22})_v$, unambiguously shows that multicomponent effects must be accounted for in modeling transport in protein crystal growth. Comparison of the present results for NH_4Cl to those for NaCl clearly shows the importance of the supporting electrolyte.

Acknowledgements

The authors thank Pamela Bowman for her considerable help in performing a literature search for this project. The support of the NASA Biotechnology Program through grant NAG8-1356 is gratefully acknowledged. A small portion of the work of D.G.M. was performed under the auspices of the US Department of Energy, Office of Basic Energy Sciences, at Lawrence Livermore National Laboratory under Contract No. W-7405-ENG-48.

References

[1] S. Miyashita, H. Komatsu, Y. Suzuki, T. Nakada, J. Crystal Growth 141 (1994) 419.
[2] K. Kurihara, S. Miyashita, G. Sazaki, T. Nakada, Y. Suzuki, H. Komatsu, J. Crystal Growth 166 (1996) 904.
[3] H. Lin, F. Rosenberger, J.I.D. Alexander, A. Nadarajah, J. Crystal Growth 151 (1995) 153.
[4] P.G. Vekilov, L.A. Monaco, B.R. Thomas, V. Stojanoff, F. Rosenberger, Acta Crystallogr. Sect. D 52 (1996) 785.
[5] F. Rosenberger, J. Crystal Growth 76 (1988) 618.
[6] M.L. Grant, D.A. Saville, J. Crystal Growth 108 (1991) 8.
[7] M. Pusey, R. Naumann, J. Crystal Growth 76 (1986) 593.
[8] L.J. Gosting, Measurement and Interpretation of Diffusion Coefficients of Proteins, in: M.L. Anson, K. Bailey, J.T. Edsall (Eds.), Advances in Protein Chemistry, Academic Press, New York, 1956, p. 429.
[9] D.G. Miller, V. Vitagliano, R. Sartorio, J. Phys. Chem. 90 (1986) 1509.
[10] O. Annunziata, L. Paduano, J.G. Albright, D.G. Miller, A.J. Pearlstein, J. Am. Chem. Soc. 122 (2000) 5916.
[11] L.A. Woolf, D.G. Miller, L.J. Gosting, J. Am. Chem. Soc. 84 (1962) 317.
[12] J.G. Albright, R. Mathew, D.G. Miller, J. Phys. Chem. 91 (1987) 210.
[13] D.G. Leaist, L. Hao, J. Chem. Soc. Faraday Trans. 89 (1993) 2775.
[14] J.G. Albright, O. Annunziata, D.G. Miller, L. Paduano, A.J. Pearlstein, J. Am. Chem. Soc. 121 (1999) 3256.
[15] M.M. Ries-Kautt, A.F. Ducruix, J. Biol. Chem. 264 (1989) 745.
[16] D.F. Rosenbaum, A. Kulkarni, S. Ramakrishnan, C.F. Zukoski, J. Chem. Phys. 111 (1999) 9882.
[17] M.L. Broide, T.M. Tominc, M.D. Saxowsky, Phys. Rev. E 53 (1996) 6325.
[18] D.G. Miller, V. Vitagliano, J. Phys. Chem. 90 (1986) 1706.
[19] A.D. Cadman, R. Fleming, R.H. Guy, Biophys. J. 37 (1981) 569.
[20] J.G. Albright, J.P. Mitchell, D.G. Miller, J. Chem. Eng. Data 39 (1994) 195.
[21] L.-O. Sundelöf, Ark. Kemi. 20 (1963) 369.
[22] V. Vitagliano, R. Sartorio, S. Scala, D. Spaduzzi, J. Solution Chem. 7 (1978) 605.
[23] J.S. Kirkaldy, G.R. Purdy, Can. J. Phys. 47 (1969) 865.
[24] T.O. Ziebold, R.E. Ogilvie, Trans. Metall. Soc. AIME 239 (1967) 942.
[25] P.Y. Lo, A.S. Myerson, AIChE J. 35 (1989) 676.
[26] E.W. Washburn (Ed.), International Critical Tables. Vol. V, McGraw-Hill, New York, 1929, p. 13.
[27] C. Tanford, M.L. Wagner, J. Am. Chem. Soc. 76 (1954) 3331.
[28] T. Arakawa, S.N. Timasheff, Biochemistry 23 (1984) 5912.